Diamond & Related Materials 18 (2009) 918–922

Contents lists available at ScienceDirect

Diamond & Related Materials

journal homepage: www.elsevier.com/locate/diamond

Adsorption of fetal bovine serum on H/O-terminated diamond studied by atomic force microscopy

B. Rezek [a,*], E. Ukraintsev [a], L. Michalíková [a], A. Kromka [a], J. Zemek [a], M. Kalbacova [b]

[a] Institute of Physics, Academy of Sciences of the Czech Republic, Cukrovarnická 10, 16253 Prague 6, Czech Republic
[b] Institute of Inherited Metabolic Disorders, 1st Faculty of Medicine, Charles University, Ke Karlovu 2, 12852 Prague 2, Czech Republic

ARTICLE INFO

Available online 14 February 2009

Pacs:
81.05.Uw
87.14.E-
87.64.Dz
87.85.J-
87.17.Rt

Keywords:
Diamond
Proteins
Atomic force microscopy
Biomaterials
Cell adhesion

ABSTRACT

We investigate adsorption of fetal bovine serum (FBS), a crucial component for cell growth, on intrinsic CVD mono-crystalline diamond with hydrogen and oxygen surface terminations. The surface terminations are prepared by oxygen and hydrogen plasma process. The FBS adsorption is done by immersing diamond into McCoy's 5A medium supplemented with 15% FBS for 10 s–24 h. After rinsing the samples are characterized in the McCoy's medium and for comparison also in air by atomic force microscopy (AFM). By optimized measurements of AFM topography in oscillating regime and by using advanced AFM regimes such as phase imaging, nanoshaving, and force spectroscopy we characterize FBS thickness, adhesion, conformation and selectivity on the H/O-diamond surfaces. We find that FBS is adsorbed in about the same monolayer thickness (2–4 nm) on both H/O-diamond surfaces, yet the protein conformation is different. We present a schematic model.

1. Introduction

Unique combination of chemical and bio-compatible properties [1,2] with mechanical and semiconducting properties has made diamond an attractive material for merging solid state and biological systems [3,4]. Hardness and low coefficient of friction make diamond attractive for bone surgery and joint replacement. Diamond bio-compatibility and resistance to chemical corrosion may increase lifetime of stents, joints, and other implants in the human body. It is also possible to make a chemical functionalization of diamond surface and create bio-passive or bio-active patterns. It was shown that hydrophobic H-terminated diamond surfaces are less favorable for osteoblast-like cell adhesion and growth than hydrophilic O-terminated surfaces [2]. This is in agreement with observations on other materials [5]. Moreover, when microscopic H/O-patterns are prepared on the same sample, the cells strongly prefer regions with O-termination (hydrophilic) compared to H-termination (hydrophobic) [6]. This is an interesting feature for tissue engineering and bio-electronics. A question remained though to what degree the cell adhesion and selectivity is influenced by the FBS adsorption. FBS contains crucial components for the cell growth (growth factors, hormones, cytokines). Without FBS in McCoy's 5A medium the cells can survive for few hours but will die during further cultivation. When cells were applied on the diamond surface in McCoy's medium without FBS, cell attachment on H- and O-terminated patterns was not selective. [6] Therefore, the direct effect of diamond surface dipoles on the cell selectivity can be excluded. The selectivity of the cells must be driven by differences in FBS adsorption on H/O-diamond surfaces.

Therefore, in this work, adsorption of FBS on hydrogen and oxygen terminated diamond surfaces was investigated by atomic force microscopy (AFM) in solution as well as in air. By optimizing measurements of AFM topography in oscillating regime and by using advanced AFM regimes such as phase imaging, nanoshaving, and force spectroscopy we characterize FBS thickness, adhesion, conformation and selectivity on the H/O-diamond surfaces. We deduce a schematic model of FBS adsorbed on H/O-diamond and discuss implications for the selectivity of cells when incubated on such surfaces.

2. Experimental

Synthetic bulk monocrystalline (MCD) intrinsic (undoped) IIa CVD diamonds (Element 6) were used as substrates. Substrates were initially cleaned by chemical cleaning in acids (97.5% H_2SO_4 + 99% powder KNO_3) at 200 °C for 30 min. Diamond surfaces were H-terminated in hydrogen microwave plasma (800 °C, 30 mbar, 1100 W, 8 min). They were cooled down in hydrogen atmosphere. Surfaces were oxidized by rf oxygen plasma process (300 W, 3 min). We prepared also H/O-diamond patterns using lithographic masks.

* Corresponding author.
E-mail address: rezek@fzu.cz (B. Rezek).

0925-9635/$ – see front matter © 2009 Elsevier B.V. All rights reserved.
doi:10.1016/j.diamond.2009.02.009

Proteins were adsorbed on MCD from 15% FBS solution (PAA) in McCoy's 5A medium with stable Glutamine without Phenolred (BioConcept). The main component of the serum is bovine serum albumin (BSA), a globular protein with typical size of 4 x 4 x 14 nm. The serum is heat inactivated (56 °C, 25 min) to destroy the immunological components yet preserve the protein. 30 μl droplet of this solution was applied on diamond surface for various periods of time (from 10 s to 24 h). Typical duration was 10 min. All experiments were performed at room temperature. This droplet was removed using two different procedures: a) rinsing with McCoy's medium without any FBS and measuring in this medium as well, so sample was always wet (this situation is the most similar to situation *in vitro* with cells), b) rinsing with water first and after that with an air blow. Eventually, samples prepared by procedure a) were further rinsed by water and blown dry by compressed air to compare the measurements in solution and in air on one sample.

AFM measurements were performed on NT-MDT NTEGRA AFM in air, water and McCoy's solutions using silicon cantilevers with force constants between 0.02 and 40 N/m. Surface topography and phase images were studied in oscillating AFM regime with set-point ratio 50% from free oscillation amplitude. The free amplitude was about 60 nm in both air and liquid. The parameters were optimized not to influence the soft FBS layer yet to provide optimal resolution and contrast.

To measure FBS layer height the FBS was removed from 2 x 2 μm area using contact mode AFM measurements with applied force around 600 nN (so called nanoshaving [4]) and remeasured in oscillating AFM regime. Step-like force increase during contact mode AFM was applied to find the threshold for FBS removal [4,7,8]. The FBS layer height was determined as the difference between average height values across 1 μm^2 of the FBS layer surface and 1 μm^2 of the nanoshaved area where FBS was removed. Several regions were probed on each sample to determine the error bar from root-mean-square (RMS) roughness values and statistical errors.

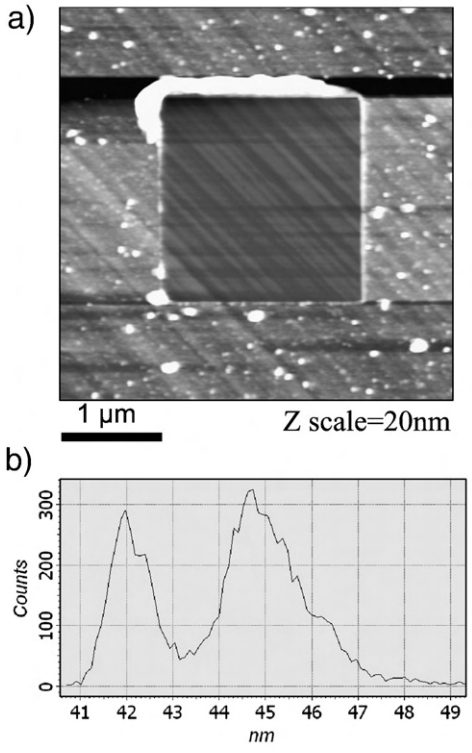

Fig. 1. (a) Typical result of AFM nanoshaving procedure of FBS layers on diamond. In this particular case, it was performed in air on oxidized diamond surface. The image was measured in oscillating AFM mode, the central area was scanned before by contact mode AFM with the applied force of 600 nN. (b) Corresponding histogram of heights.

Table 1
The thicknesses of FBS layer on mono-crystalline diamond obtained by AFM in air and McCoy's solution.

Surface rinsing	AFM measuring	FBS layer thickness, nm	
Medium	Medium	H-term. diamond	O-term. diamond
McCoy	McCoy	1.5 ± 2	2 ± 2
McCoy	Air	3 ± 2	3 ± 2
Water	Air	4 ± 2	3 ± 2

FFT filtering was used on detail topography measurements to remove polishing marks on the surface. Typical RMS value for MCD samples is 0.6 nm at 1 μm^2 area, it is reduced to 0.1 nm after the FFT filtering. Autocorrelation function (ACF) was calculated from the topography images to determine typical lateral feature size (Lx). The Lx parameter corresponds to such distance, at which ACF decreases by e times, i.e. $ACF(0)/ACF(Lx) = e$.

Force spectroscopy measurements [9] were performed in liquid using soft cantilevers with nominal force constant of $k = 0.05$ N/m. Force of 20 nN was applied during approach to catch the protein molecules on the surface. A cantilever was retracted from the surface with the speed of ≈ 1 μm/s.

XPS analysis was performed on a photoelectron spectrometer ADES 400 (VG Scientific, UK) equipped with Al and Mg twin anode X-ray source and a hemispherical rotatable electron energy analyzer. Photoelectrons were excited by Mg Kα radiation (1253.6 eV, 10 keV, 20 mA). Photoelectron spectra were corrected for surface charging with respect to the C 1 s line peaked at 285.3 eV. Inelastic electron background was subtracted using the Shirley's procedure.

3. Results

Fig. 1 shows a typical result of AFM nanoshaving procedure of FBS layers on diamond. In this particular case, it was measured in air on oxidized diamond surface. The histogram in Fig. 1(b) displays two distinct peaks from which the FBS layer height (peak separation) as well as RMS roughness (peak width) can be resolved. The thickness values for both types of surfaces after different rinsing procedures and in different media are summarized in Table 1.

The data show that the FBS layer is present on both types of diamond surfaces in about similar thickness. When measured in liquid, FBS layer height is slightly smaller (1.5 ± 2 nm) on H-terminated diamond compared to O-terminated diamond (2 ± 2 nm). When measured in air, the heights are about 3 nm on both H- and O-diamond. AFM resolution in Z direction is < 0.1 nm and it is much smaller than the error bars given. The layer height values are not affected by the AFM tip shape. All values are comparable with the typical cross-section of the BSA

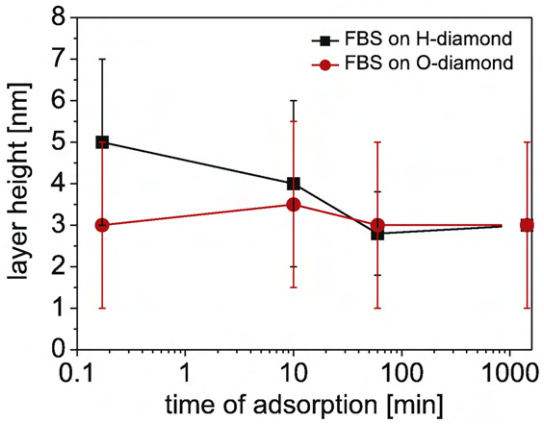

Fig. 2. FBS layer thickness as a function of FBS adsorption time on H- and O-terminated diamond.

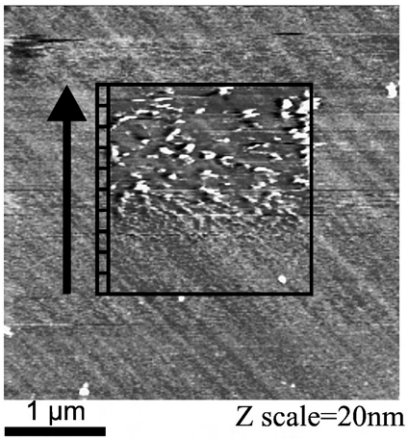

Fig. 3. Oscillating mode AFM image of AFM nanoshaving procedure in solution for determining the threshold of FBS removal from O-terminated diamond surface. The arrow denotes the direction of AFM nanoshaving in the central area, small black squares denote 2.5 nN steps in the AFM tip loading force, starting from 2.5 nN. The threshold is determined at 10 nN in this case.

protein (4×4 nm). This suggests that the proteins must be laying on the surface. Note that rinsing by water gives similar results as rinsing by McCoy's medium, i.e. McCoy's medium has no specific effect on the result due to its composition.

The result that the FBS layer in air is thicker than the same layer in liquid was confirmed on several samples. All experiments show similar results. Layer height in air may differ slightly (2–5 nm), but layer height in solution is always 0.5–2 nm smaller than in air. The ratio $height(liquid)/height(air)$ is about 0.5–0.8. We also performed experiments on H/O-termination micro-patterns with the same outcome.

Fig. 2 shows the FBS layer thickness in air as a function of FBS adsorption time. The FBS layer thickness practically does not depend on time of adsorption in the range of 10 s–24 h on the particular type of surface. The FBS adsorbs in a full layer thickness within 10 s, this is very fast compared to typical cell adsorption times in the range of tens of minutes.

Fig. 3 shows the actual threshold for removing the FBS layer from the O-diamond surface by contact AFM in solution. The arrow denotes the direction of AFM nanoshaving, small black squares denote 2.5 nN steps in the AFM tip loading force, starting from 2.5 nN. The threshold is determined at 10 nN in this case. Similar data were obtained also on H-terminated surface (not shown) with the threshold of 5 nN. The experiment was performed with the same tip. Similar measurements were performed also in air with the same outcome.

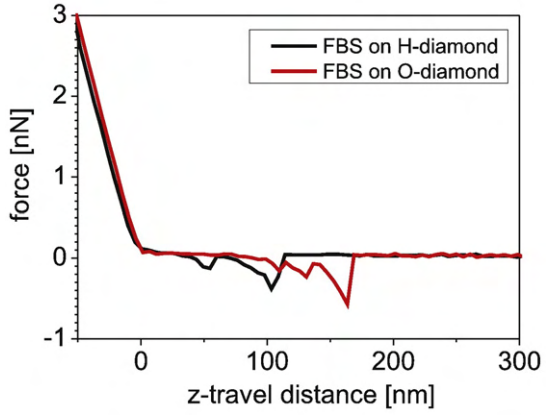

Fig. 4. AFM force curves exhibiting the features corresponding to protein stretching on both H- and O-terminated diamond.

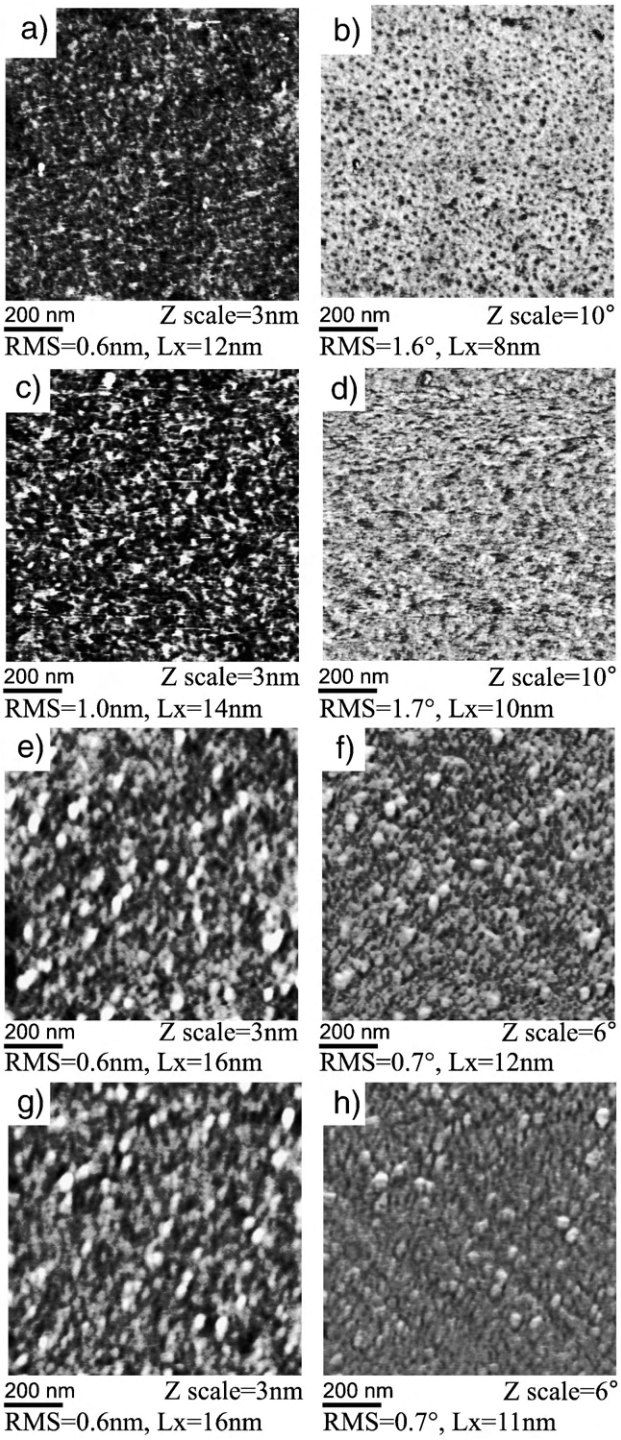

Fig. 5. AFM topography and phase measurements of MCD surfaces with adsorbed FBS layers in different conditions with corresponding RMS and Lx values: topography and phase in liquid on (a–b) FBS/H-diamond (c–d) FBS/O-diamond, topography and phase in air on (e–f) FBS/H-diamond (g–h) FBS/O-diamond.

The removal thresholds forces correspond to a non-covalent bond of FBS to the diamond [4,8]. The difference by a factor of two can be attributed to a higher stiffness of the FBS layers on O-diamond. Higher stiffness can be interpreted as a denser packing of the FBS layer. This deduction is corroborated also by XPS experiments. XPS detection of nitrogen, which is present in the organic molecules, shows 5.8 ± 0.4 and 6.7 ± 0.5 at.% on H-diamond and O-diamond, respectively. Hence XPS data show somewhat higher nitrogen content on O-diamond. No nitrogen was detected prior to FBS adsorption.

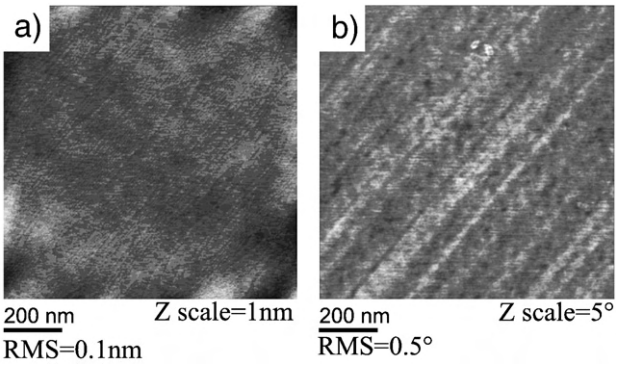

Fig. 6. AFM topography and phase measurements of a bare diamond surface with corresponding RMS values.

Fig. 4 shows force curves obtained by force spectroscopy on H- and O-terminated diamond. The force curves exhibit 500 ± 100 pN interaction between tip and surface on both H- and O-terminated diamond. The same forces were found between BSA-functionalized cantilever and glass surface after deposition of proteins [9]. The stretching length of 200 nm is also similar to the previously reported results [9]. Note that the stretching was observed for 10% of curves, 90% showed no interaction. Low percentage is quite common because the AFM tip does not always catch the molecules. This means that hardly any conclusion can be made about the actual protein density based on these measurements. Nevertheless, the shape of the force curves proves that one or more protein molecules were stretched. Hence the protein molecules are present on both H- and O-diamond.

Fig. 5 shows detailed topography and phase images of FBS layers on H/O-diamonds in liquid and in air. Values of RMS roughness and Lx (lateral feature size) are also given. When measured in McCoy's medium, lateral feature size in topography is similar (12–16 nm), with a kind of ridge-like shape. The lateral size is in a good agreement with the protein length (14 nm). The Lx can be overestimated by the tip shape. However, it does not really matter for the comparison. The Lx is about the same in all cases. Similar is also RMS of the phase images (1.6°). Yet there are also distinct differences between the FBS layers in McCoy's medium: the roughness of FBS on O-diamond (1.0 nm) is about two times higher compared to H-diamond (0.6 nm). AFM phase image of FBS on H-diamond shows clear dark dots correlated with protrusions in morphology while on O-diamond it is rather blurred. When the measurements are done in air the morphology and phase images change significantly, there are hillocks on the surface and the phase shows brighter features surrounded by darker boundaries. This appearance and also roughness (0.6 nm) are the same for FBS on both H- and O-diamond. Note that the protein adsorption procedure was the same, the protein appearance changes only due to the change of the measurement medium (liquid vs. air). For comparison a bare diamond substrate is also measured as shown in Fig. 6. No special features are resolved there except for typical polishing marks. Note that RMS values generally depend on a tip shape, yet the observed differences were similar using several cantilevers and samples.

4. Discussion

The FBS adsorbed on both H- and O-terminated diamond surface. This is in agreement with previous reports that albumin [10] and also fibronectin [11] adsorb on both hydrophilic and hydrophobic surfaces. The FBS layers characterized by AFM in the medium exhibit different surface roughness, phase images, and slightly different thickness on H- and O-diamond. However, these differences between the layers on H- and O-diamond disappear when measured in air on the same samples. Moreover, the FBS layer is significantly thicker in air than in liquid. One may argue that within the error bar, there are no differences in protein layer heights. However, AFM images clearly show different morphology and phase. This indicates that the protein arrangement must be different on the H/O surfaces. Therefore, we think that it is plausible to discuss also the small differences of height, even though they are within the error bar. To explain the observation we propose the model how the proteins are organized on diamond surfaces and how AFM probes these protein layers. The model is schematically shown in Fig. 7.

In the schematic model, the oval shape (green) denotes hydrophobic parts of the protein. The black dots around denote hydrophilic parts. The horizontal line (red) denotes the surface which is sensed by AFM. The protein adsorbs with hydrophobic part to the hydrophobic H-diamond and stretches hydrophilic parts into the solution. On O-diamond the protein's hydrophobic core remains surrounded by hydrophilic parts. This is in agreement with general mechanism of protein adsorption on hydrophobic and hydrophilic surface [10]. Yet here the observed differences are much less pronounced. We propose that in solution the hydrophilic parts above the protein are solvated and quite flexible and hence not directly sensed by AFM (in spite of reducing the tip-surface interaction as much as possible). Therefore, we observe different thickness and roughness of the layers on H/O-diamond. The different phase images also corroborate the different arrangement of proteins as shown in the model. When the sample is in air, the solvated parts collapse on the surface. AFM then detects FBS layers with the same thickness, roughness, and phase images on both H- and O-diamond substrates.

These differences in protein arrangement can lead to different cell adhesion properties [5] and consequently also to selective cells growth on H/O-diamond patterns [6]. However, one has to critically consider that the composition of the adsorbed layers may be different on H- and O-diamond, because various proteins from FBS influence cell adhesion in different ways [12,13]. It is also known that protein adsorption is a competitive process between different proteins [14]. Very similar thickness, force curve features, and XPS on both H/O-diamond nevertheless indicate that also the composition of the layers is very similar. Only the difference in nanoshaving threshold by a factor of 2 indicates slight difference in the FBS layer density.

By comparison with the literature [5,10] it seems that the most important factor for the cell growth on diamond is the wetting property of the surface rather than any specific property of diamond.

5. Conclusions

Comparing the data obtained by AFM, phase imaging, nanoshaving, and force spectroscopy we conclude that the FBS proteins are

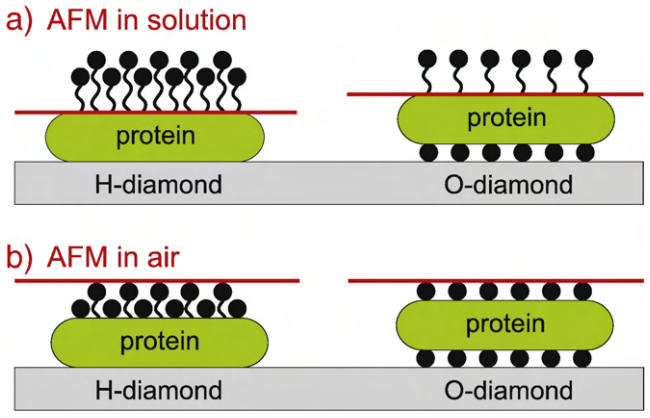

Fig. 7. Schematic model of FBS proteins on H/O-diamond surfaces (a) in solution and (b) in air. The oval shape (green) denotes hydrophobic parts of the protein. The black dots around denote hydrophilic parts. The horizontal line (red) denotes the surface which is sensed by AFM.(For interpretation of the references to colour in this figure legend, the reader is referred to the web version of this article.)

present on both H/O-diamond surfaces. They are laying on the surface in about a monolayer coverage and do not form covalent bonds to the diamond surface with either H- or O-termination. While in air we could not resolve any differences, the different FBS layer roughness and different features in AFM phase images indicate different configuration of proteins on H/O-diamond in the cell culture medium (McCoy's 5A). The nanoshaving experiments also indicate slightly higher stiffness of FBS layer on O-diamond. Those are most likely the reasons for the cell preference to O-diamond when the surface is patterned by both H and O atoms. Hence it is neither a direct effect of diamond surface dipoles on the cells or selective adsorption of proteins on H/O patterns that drives the cell selectivity, but rather the different protein conformation. The detailed influence of these differences on the mechanisms of cell adhesion and viability still remains to be elucidated. These findings are crucial for controlling formation of cell arrays on diamond in tissue engineering and bio-electronics as well as for understanding the performance of cell-diamond devices.

Acknowledgments

We would like to acknowledge the kind assistance of Ing. V. Jurka with photolithography and Z. Poláčková with chemical treatments. This research was financially supported by the projects KAN400100701 (GAAV), LC510 (MŠMT), LC06040 (MŠMT), AV0Z10100521, MSM0021620806 (MŠMT), and by the Fellowship J.E. Purkyně.

References

[1] L. Tang, C. Tsai, W. Gerberich, L. Kruckeberg, D. Kania, Biomaterials 16 (6) (1995) 483.
[2] M. Kalbacova, M. Kalbac, L. Dunsch, A. Kromka, M. Vanecek, B. Rezek, U. Hempel, S. Kmoch, Phys. Status Solidi, B 244 (11) (2007) 4356.
[3] W. Yang, J. Butler, J.J.N. Russell, R. Hamers, Langmuir 20 (2004) 6778.
[4] B. Rezek, D. Shin, C.E. Nebel, Langmuir 23 (2007) 7626.
[5] K. Anselme, Biomaterials 21 (2000) 667.
[6] M. Kalbacova, L. Michalíková, V. Barešová, A. Kromka, B. Rezek, S. Kmoch, Phys. Status Solidi, B 245 (2008) 2124.
[7] B. Rezek, D. Shin, T. Nakamura, C.E. Nebel, J. Am. Chem. Soc. 128 (2006) 3884.
[8] B. Rezek, D. Shin, H. Uetsuka, C.E. Nebel, Phys. Status Solidi, A 204 (2007) 2888.
[9] C. Popov, W. Kulisch, J. Reithmaier, T. Dostalova, M. Jelinek, N. Anspach, C. Hammann, Diam. Relat. Mater. 16 (2007) 735.
[10] M.M. Browne, G.V. Lubarsky, M.R. Davidson, R.H. Bradley, Surf. Sci. 553 (2004) 155.
[11] G. Altankov, F. Grinnell, T. Groth, J. Biomed. Mater. Res. 30 (1996) 385.
[12] X.-S. Cui, Y.-J. Jeong, H.-Y. Lee, S.-H. Cheon, N.-H. Kim, Reproduction 124 (2004) 125.
[13] Y. Arima, H. Iwata, J. Mater. Chem. 17 (2007) 4079.
[14] S.R. Sousa, M. Lamghari, P. Sampaio, P. Moradas-Ferreira, M.A. Barbosa, Wiley Periodicals, Inc. doi:10.1002/jbm.a.31201.